Paper accepted for presentation at 2009 IEEE Bucharest Power Tech Conference, June 28th - July 2nd, Bucharest, Romania

Control of Hybrid Fuel Cell Generation Systems for Voltage Sag Ride-Through Studies

A.Hajizadeh, M.A.Golkar, L.Norum

Abstract-- This paper proposes the power management strategy of a hybrid fuel cell distributed generation system includes solid oxide fuel cell and battery energy storage during the voltage disturbances in distribution systems. As the power generated by DG units increases, the behavior of DG units subjected to voltage sags must be carefully considered to avoid power unbalance, which may turn into instability. However to achieve a sustainable grid reliability combined with large penetration of DG, some gird operators already require voltage sag ride-through capability. Hence, the proposed control strategy allows the hybrid distributed generation system operate properly during the occurring the voltage sags in distribution systems. Simulation results are given to show the overall system performance including active power control and voltage sag ride-through capability of the hybrid distributed generation system.

Index Terms-- **Battery, Fuel Cell, Hybrid Distributed Generation, Fuzzy Control, Lyapunov Stability.**

I. Introduction

Nowadays, the traditional centralized generation is slowly changing to a new paradigm, driven by environmental considerations and by the flexibility of the topology. This new model, usually known as distributed or embedded generation is characterized by the small generation size, the proximity to the loads, and its connection to distribution networks. Fuel cells have attracted much attention as an efficient, scalable, low-pollution means of generation electrical power [1]. However, limited by their inherent characteristics such as a long start-up time and poor response to instantaneous power demands, hybrid fuel cell/battery distributed generation systems have been presented to reach the high power density of batteries with the high energy density of fuel cells [2,3]. The effect of load transients and disturbances can be reduced by combining the fuel cells with energy storage devices such as capacitors or batteries to form a hybrid system. In case of grid-connected operation of hybrid fuel cell systems, these systems can be placed in distribution systems to support the utility grid. Pulse width modulation (PWM) voltage source converters (VSCs) are used to connect these hybrid systems to distribution systems and this interface is highly sensitive to grid disturbances such as voltage sags. Voltage sags are momentary decreases in rms voltage caused by a short-duration increase in grid current originating from motor starting, transformer energizing or faults in the electric supply system. Voltage sags have been proven to be one of the most important aspects of power quality [4]. The operation of hybrid fuel cell distributed generation system is very important during voltage sag and it needs the control strategy to keep the stability of the system, manage of power between the components of the hybrid fuel cell system and deliver the power to load. Up to now various control structure have been proposed for hybrid fuel cell systems, which are aimed at improving the power flow under load transient conditions [5]. But the operation control of hybrid fuel cell distributed generation system during voltage sag has not been considered. Hence, this paper presents an optimal control strategy for hybrid fuel cell/battery distributed generation system. For this purpose, the neuro-fuzzy control strategy is introduced to manage the power flow between power sources of the hybrid system. Based on the dynamic modeling of the hybrid system, local controllers are designed to regulate the operating point of each component.

II. System Description

In this paper, a grid connected HDGS is evaluated. Hybrid fuel cell distributed generation systems, like any DC generating system, need an electronic converter to interface with the AC system. In DG applications, the converter is connected in parallel with the network, in the same way a traditional generator is connected. Fig.1 shows the block diagram of the HDGS proposed in this paper. As shown in the figure, it consists of a fuel cell, a battery, DC to DC power converters, a 3-phase DC to AC inverter and an output filter. The mathematical models describing the dynamic behaviour of each of these components are given in [5- 6].

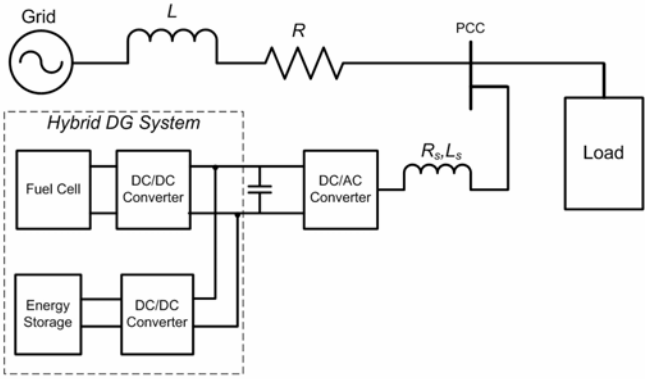

Fig.1 The structure of proposed hybrid DG system

A.Hajizadeh and M.A. Golkar are with the Electrical Engineering Department, K.N. Toosi University of Technology, Tehran, Iran. *Email address: aminhajizadeh@ee.kntu.ac.ir, golkar@eetd.kntu.ac.ir*

L.Norum is with the Energy Conversion Group of Electric Power Engineering Department, Norwegian University of science and Technolog, Trondheim, Norway. *Email address: norum@ntnu.no.*

978-1-4244-2235-7/09/$25.00 ©2009 IEEE

III. Power Flow Control of Hybrid DG System During Voltage Sag

In this section, the control strategy of the hybrid fuel cell/battery distributed generation system has been presented. The overall control structure is illustrated in Fig.2, which includes the power flow controller and local controllers for power conditioning units and the fuel cell. The term, "power flow control", refers to the design of the higher-level control algorithm that determines the proper power level to be generated, and its split between the two power sources. The power flow control strategy is designed to determine the proper power level between the fuel cell stack and battery energy storage, while satisfying the power demand from the load and maintaining adequate energy in the energy storage device. Frequent power demand variations and unpredictable load profile are unavoidable uncertainties. Also, nonlinear and often time-varying subsystems add to the complexity of the structure of a hybrid system. Moreover, the control strategy must work real time to distribute the power between power sources based on the system conditions. Hence real time control strategy based on fuzzy logic has been proposed for instantaneous power management [5]. But the parameters of the proposed fuzzy controller during the power management have been considered constantly and it has not the adaptive property. To improve the performance of the power flow control strategy, the optimal fuzzy control strategy is proposed. In this control structure, the fuel cell power is determined optimally according to the demand power (P_{demand}), the magnitude of grid voltage (v_{grid}), the battery power (P_{batt}), the battery's state of charge (SOC) and the fuel cell power in one time step ago ($P_{fc}(k-1)$). To generate the fuel cell power optimally, the efficiency maps of the fuel cell and battery energy storage are used. As shown in Fig.2, the maximum efficiency of the fuel cell is at the level power between 20kW and 30kW. According to the Fig.3, the maximum efficiency of the battery during the charge and discharge cycles, is around the state of charge of 75%. Moreover, in order to operate the fuel cell stack at an optimal fuel utilization point, the fuel cell controller is to maintain an optimal hydrogen utilization, Uf,opt, around 85% [7]. During the voltage sags, the power flow control strategy must be designed to manage the power between the dual power sources and the utility grid. It is proven that there is a direct proportionality between the maximum current of voltage source converter and the value of the actual input power to dc bus [6].

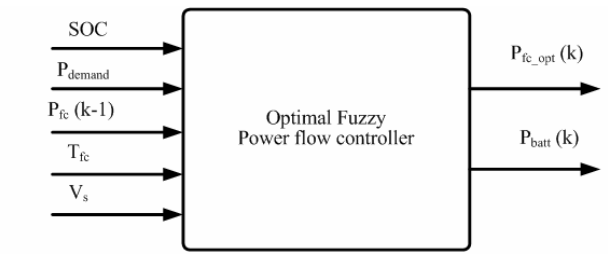

Fig.2 Power Flow control structure

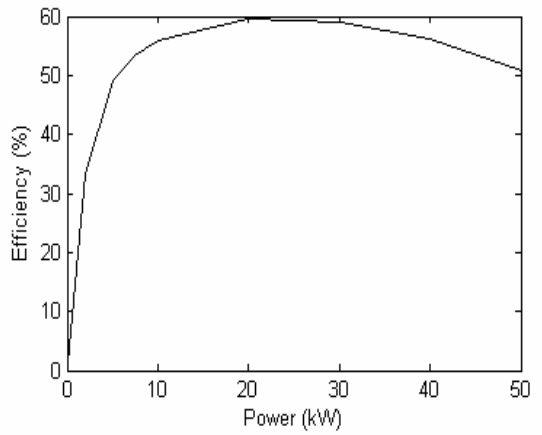

Fig.3 Efficiency map of fuel cell stack

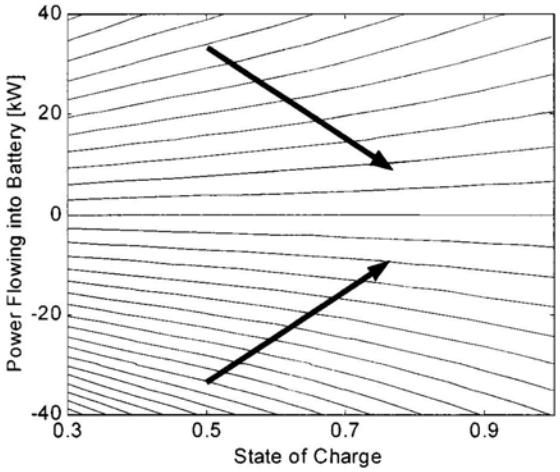

Fig. 4 Charge and discharge diagrams of battery

In other words, if the input power to dc bus is lowered by the ratio K, the maximum value of the current will also be lowered by the same ratio. To calculate the required current rating of the voltage source converter switches to ride-through voltage sags at the grid, the maximum current has been calculated for single phase faults (sag type B and D) with zero phase angle jump as:

$$I_{\max} = \sqrt{\frac{2}{3}} . \frac{KP_{dc}}{e_{dp} + e_{dn}} \quad (1)$$

While for two phase faults (sag types C, E, F, G) it is given by

$$I_{\max} = \sqrt{\frac{2}{3}} . \frac{KP_{dc}}{e_{dp}^2 - e_{dn}^2} \sqrt{\frac{1}{4}(e_{dp} - e_{dn})^2 + \frac{3}{4}(e_{dp} + e_{dn})^2} \quad (2)$$

For the three phase faults (sag type "A"), the maximum phase current is:

$$I_{\max} = \sqrt{\frac{2}{3}} . \frac{KP_{dc}}{E \times V_{dip}} \quad (3)$$

Where K is the ratio of the input power actually delivered to dc link. The values of e_{dp} and e_{dn}, which are the positive and negative sequence of the d-component of the grid voltage for different voltage sags with E the phase-to-phase RMS grid voltage, V_{sag} the sag magnitude. Note that since the sags have zero phase angle jump, the d-components correspond to the magnitudes of their sequence voltages. Therefore, if the

converter switches have to be rated to ride through all sags with 30% minimum magnitude, the current rating can be decreased from about 3.5 p.u. to 3 p.u., if the input power is decreased from 90% to 70% of nominal value. Because of the slow variations of the SOFC power, it is important to change the reference power of the battery bank for decreasing the input power to dc bus during voltage disturbances. Under this condition, a part of the power which not delivers by hybrid distributed generation system to the load is provided from the utility grid. Also, fuel cell power must change smoothly so that the fuel cell operating point deviation is minimized and the fuel cell temperature does not increase out of the desired limit. In this case, both battery and fuel cell system contribute to providing dc bus power.

$$P_{dc\_bus}(t) = P_{batt}(t) + P_{fc}(t) \qquad (4)$$

A Fuzzy Logic Controller (FLC) is used to decide the operating point of the fuel cell stack. It is necessary to determine the fuel cell stack optimal power to assist the battery in charge or discharge modes. It follows the idea of load leveling, where the battery is used to provide assisting or generating, while operating the fuel cell at an optimum. A fuzzy logic controller determines the controller output based on the inputs using a list of if-then statements called rules. The if-part of the rules refers to adjectives that describe regions (fuzzy sets) of the input variables. A particular input value belongs to these regions to a certain degree, so it is represented by the degree of membership. To obtain the output of the controller, the degrees of membership of the if-parts of all rules are evaluated, and the then-parts of all rules are averaged and weighted by these degrees of membership. The core of the rule set of the fuzzy controller is illustrated as follows.

(1) Battery Charge Mode

Rule 1: if V_{grid} is normal and P_{demand} is Low and SOC is Low and T_{fc} is Low and P_{batt}(k-1) is Negative High and P_{fc}(k-1) is Low then P_{fc}(k) is Medium.

Rule 2: if V_{grid} is normal and P_{demand} is Medium and SOC is Low and T_{fc} is Low and P_{batt}(k-1) is Negative Medium and P_{fc}(k-1) is Medium then P_{fc}(k) High.

Rule 3: if V_{grid} is normal and P_{demand} is Medium and SOC is Low and T_{fc} is High and P_{batt}(k-1) is Negative Low and P_{fc}(k-1) is Medium then P_{fc}(k) is High.

(2) Hybrid Mode

Rule 4: if V_{grid} is normal and P_{demand} is Medium and SOC is High and T_{fc} is Low and P_{batt}(k-1) is Low and P_{fc}(k-1) is Low then P_{fc}(k) is Medium.

Rule 5: if V_{grid} is normal and P_{demand} is Medium and SOC is High and T_{fc} is Low and P_{batt}(k-1) is Medium and P_{fc}(k-1) is Medium then P_{fc}(k) is Medium.

Rule 6: if V_{grid} is normal and P_{demand} is Medium and SOC is High and T_{fc} is High and P_{batt}(k-1) is Medium and P_{fc}(k-1) is Medium then P_{fc}(k) is Low.

Rule 7: if V_{grid} is normal and P_{demand} is High and SOC is High and T_{fc} is Low and P_{batt}(k-1) is Low and P_{fc}(k-1) is Medium then P_{fc}(k) is High.

Rule 8: if V_{grid} is normal and P_{demand} is High and SOC is High and T_{fc} is Low and P_{batt}(k-1) is Medium and P_{fc}(k-1) is Low then P_{fc}(k) is Medium.

Rule 9: if V_{grid} is normal and P_{demand} is High and SOC is High and T_{fc} is High and P_{batt}(k-1) is Medium and P_{fc}(k-1) is High then P_{fc}(k) is Medium.

Rule 10: if V_{grid} is normal and P_{demand} is High and SOC is High and T_{fc} is High and P_{batt}(k-1) is High and P_{fc}(k-1) is Medium then P_{fc}(k) is Low.

Rule 11: if V_{grid} is normal and P_{demand} is High and SOC is Low and T_{fc} is Low and P_{batt}(k-1) is Low and P_{fc}(k-1) is Medium then P_{fc}(k) is High.

(3) Battery Operation Mode

Rule 12: if V_{grid} is normal and P_{demand} is Low and SOC is High then P_{fc}(k) is Zero.

(4) Voltage Disturbance Mode

Rule 13: if V_{grid} is abnormal then $P_{fc}(k) = P_{fc}(k-1)$.

In this condition the battery power command is negative and calculated as follow:

$P_{batt}(k) = P_{dc\_bus}(k) - P_{fc}(k)$;

$P_{dc\_bus}(k) = K \times P_{dc\_bus}(k-1)$;

K is the ratio that the dc bus power must be decreased during the voltage sag.

So, the following error function has been used for the neuro-fuzzy control strategy to train the parameters of membership functions in fuzzy controllers. This process has been explained in next section.

$$E(k) = \sum_{k=1}^{N-1} w_1 (P_{fc}(k) - P_{fc\_opt})^2 + w_2 (SOC(k) - SOC_{opt})^2 + w_3 (U_f(k) - U_{f\_opt})^2 \qquad (12)$$

Where N is the duration of the power demand and w_1, w_2 and w_3 are the weighting coefficients representing the relative importance of the objectives and they must satisfy the equation (13).

$$w_1 + w_2 + w_3 = 1 \qquad (13)$$

Recently, the combination of neural networks and fuzzy logic has received attention [8-9]. Neural networks bring into this union the ability to learn, but also require an excessive number of iterations for training of complex systems. Fuzzy logic offers a system model based on membership functions and a rule base, but requires an explicit stating of the IF/THEN rules. In this type of model, the condition part uses linguistic variables and the conclusion part is represented by a numerical value which is considered as a function of system condition expressed with the variables $x_1, x_2, \ldots, x_m$.

$$\omega^l = g(x_1, x_2, .., x_m) \qquad (14)$$

The neuro-fuzzy algorithm uses membership functions of gaussian type. With gaussian fuzzy sets, the algorithm is capable of utilizing all information contained in the training set to calculate each rule conclusion, which is different when using triangular partitions. Fig.8 illustrates the neuro-fuzzy scheme for an example with two input variables (x_1, x_2) and one output variable (y). In the first stage of the neuro-fuzzy scheme, the two inputs are codified into linguistic values by

the set of gaussian membership functions attributed to each variable.

The second stage calculates each rule $R^{(l)}$ its respective activation degree. Last, the inference mechanism weights each rule conclusion $\omega^{(l)}$, initialized by the cluster-based algorithm, using the activation degree computed in the second stage. The error signal between the model inferred value *Y* and the respective measured value (or teaching value) *y'*, is used by the gradient descent method to adjust each rule conclusion. The algorithm modifies the values of $\omega^{(l)}$ to minimize an objective function *E* usually expressed by the mean quadratic error (5). In this equation, the value *y'(k)* is the desired output value related with the condition vector $x'(k) = (x_1', x_2', \ldots x_m')$. The element *Y(x'(k))* is the inferred response to the same condition vector *x'(k)* and computed by Equation (6).

$$E = \frac{1}{2}[Y(x^{'}(k)) - y^{'}(k)]^2 \tag{5}$$

$$Y(x^{'}(k)) = \frac{\sum_{l=1}^{c}\left(\prod_{j=1}^{m}\mu_{A_{j=1}^{(l)}}(x_j^{'}(k))\right).\omega^{(l)}(k)}{\sum_{l=1}^{c}\left(\prod_{j=1}^{m}\mu_{A_{j=1}^{(l)}}(x_j^{'}(k))\right)} \tag{6}$$

Equation (6) establishes adjustment of each conclusion $\omega^{(l)}$ by the gradient-descent method. The symbol α is the learning rate parameter, and *t* indicates the number of learning iterations executed by the algorithm.

$$\omega^{(l)}(t+1) = \omega^{(l)}(t) - \alpha\frac{\partial E}{\partial \omega^{(l)}} \tag{7}$$

The inference function (5) depends on $\omega^{(l)}$ only through its numerator. The expression composing the numerator is now denoted by *a* and is shown in (8).

$$a = \sum_{l=1}^{c}\left(\prod_{j=1}^{m}\mu_{A_{j=1}^{(l)}}(x_j^{'}(k))\right).\omega^{(l)}(k) \tag{8}$$

The denominator of function (6) is dependent on a term $d^{(l)}$, defined in (19), and denoted by *b* in (10).

$$d^{(l)} = \prod_{j=1}^{m}\mu_{A_{j=1}^{(l)}}(x_j^{'}(k)) \tag{9}$$

$$b = \sum_{l=1}^{c}(d^{(l)}) \tag{10}$$

To calculate the adjustment of each conclusion value $\omega^{(l)}$, it is necessary to compute the variation of the objective function *E*, ∂E , in relation to the variation that occurred in $\omega^{(l)}$ in the anterior instant, $\partial\omega^{(l)}$. Therefore, using the chain rule to calculate $\partial E/\partial\omega^{(l)}$ results in expression (11).

$$\frac{\partial E}{\partial \omega^{(l)}} = \frac{\partial E}{\partial Y}\frac{\partial Y}{\partial a}\frac{\partial a}{\partial \omega^{(l)}} \tag{11}$$

The use of chain rule looks for the term contained in *E* that is directly dependent on the value to be adjusted, i.e., the conclusion value $\omega^{(l)}$. Therefore, we can verify by chain equation (11) that it starts with *E* dependent of *Y* value, the *Y* value depends on term α and, at last, the expression *a* is a function of $\omega^{(l)}$. After some computation, the adjustment to be made in $\omega^{(l)}$ can be interpreted as being proportional to the error between the neuro-fuzzy model response and the supervising value, but weighted by the contribution of rule *(l)*, denoted by $d^{(l)}$, to the final neuro-fuzzy inference.

$$\omega^{(l)}(t+1) = \omega^{(l)}(t) - \alpha\frac{(Y(x^{'}(k)) - y^{'}(k))d^{(l)}}{\sum_{l=1}^{c}(d^{(l)})} \tag{12}$$

IV. Controller Designs for Power Electronic Devices and Fuel Cell Stack

The final part of the control structure is the designing of the local controllers for fuel cell power plant, DC/DC converter and grid connected inverter to track the proposed set points. Each component will be controlled by its own local controller so that the subsystem is stable and the power demand is satisfied as much as possible. The details of these local controllers have been described completely in [5, 6] and only the control diagram of each component has been shown here. Fig.5.illustrates the control structure of fuel cell system. According to the error between the reference current and actual current, the output of the fuzzy logic controller is the hydrogen molar flow $q_{H_2\text{-ref}}$.

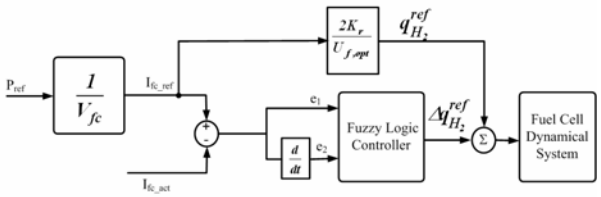

Fig.5 Fuzzy Control structure of fuel cell power plant

The unregulated output voltage of the FC is fed to the dc/dc boost converter. The voltage is boosted depending upon the duty ratio. This boosted voltage is compared with a reference dc voltage to generate an error signal. The change in error is calculated. The error and the change in error are fed as inputs to the FLC. The FLC generates control signal based upon the inputs and rule base. The control signal is fed to the PWM generator. The PWM generator based upon the control signal adjusts the pulses of the switch of the boost converter. The control structure of DC/DC converter has been presented in Fig.6. The output of DC/DC converter is connected to the input of voltage source converter.

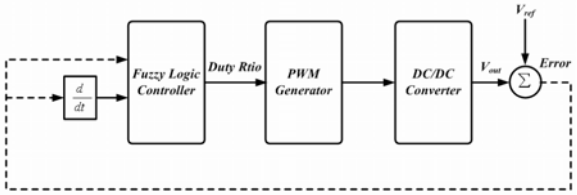

Fig.6 Fuzzy Logic Controller for DC/DC Converter

Control of grid connected voltage source converter (VSC) is an important problem during voltage disturbances like voltage sag. The VSC is connected to the grid via a filter inductor. The dq-components of currents and voltages are then used along with the reference current signals. The VSC controller is required to have main functions: Current control

and DC link voltage regulation. The current controller used here consists of two PI controllers that control the positive and negative sequence current separately and are implemented in two different rotating coordinate systems. Details on the dual sequence controller and DC link voltage regulator can be found in [6]. A simplified scheme for the dual sequence control is shown in Fig.7.

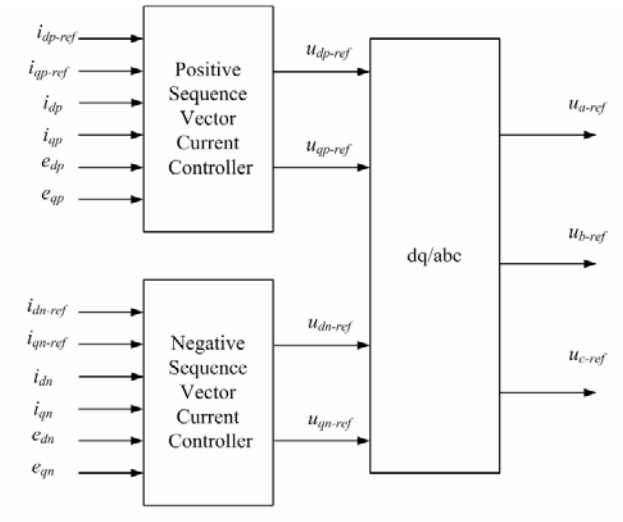

Fig.7 Proposed dual sequence current control

V. Simulation Results

In order to show the effectiveness of proposed control strategy, the simulation model of the proposed hybrid DG system has been built in Matlab/Simulink environment. The parameters of the hybrid fuel cell/ battery distributed generation system in this study are given in Table I. The battery bank operates as a buffer of energy to meet load demand that cannot be met by the FC system, particularly during transient or disturbances periods. In a hybrid fuel cell\battery energy storage system, a certain amount of power may be scheduled to be delivered to a load center from the utility grid with the rest to be supplied by the hybrid system. In this case study, the output power of the FC system is limited to 50 kW and the battery bank system is capable of sustaining the extra load of 20 kW for 100s during peak demand periods. Also it is supposed that the initial state of charge for the battery bank is 0.7. For the investigated system, simulations have been run with unbalanced voltage sag (type C) with magnitude 40%. The sag starts at 0.3sec and ends at 0.4sec. The DC-link voltage is shown in Fig.8. The grid currents increase to above 2 p.u and DC voltage shows a variation during the transients at the beginning and end of the sag. However, the ripple during the transient is not bigger than 10% peak-to-peak and is quite quickly damped to almost zero. As shown in Fig.9, the generated power of the hybrid distributed generation system is decreased to 70% of nominal value to increase the ride through capability of all sags with 30% minimum magnitude. Because of the slow variations of the SOFC, the output power of the fuel cell power plant remains constant during the voltage sag as shown in Fig.10.

TABLE I
HYBRID SYSTEM PARAMETERS

Fuel Cell System Parameters	
Faraday's constant (F)	96484600[C/kmol]
Hydrogen time constant (t_{H2})	26.1 [s]
Hydrogen valve molar constant(K_{H2})	8.43×10^{-4}
k_r Constant=$N_0/4F$	9.9497×10^{-7}
No Load Voltage (E_0)	0.6 [V]
Number of Cells (N_0)	384
Oxygen time constant (t_{O2})	2.91[s]
Oxygen valve molar constant (K_{O2})	2.52×10^{-3}
FC internal resistance *(r)*	0.126 [Ω]
FC absolute temperature *(T)*	343 [K]
Universal gas constant *(R)*	8314.47 [J/(kmol K)]
Utilization Factor *(U_f)*	0.8
Water time constant *(t_{H2O})*	78.3 [s]
Water valve molar constant *(K_{H2O})*	2.81×10^{-4}
DC/DC Converter Parameters	
Rated voltage (V)	200V/540V
Resistance (R)	2.3 [Ω]
Capacitance (C)	1.5 [mF]
Inductor (L)	415 [μH]
DC/AC Converter Parameters	
Nominal AC Voltage	400 V
Nominal phase current	100 A
Nominal DC voltage	540 V
DC-link capacitance	550 μF
R_s	23 mΩ
L_s	0.73 mH
f_s	50 Hz
Battery Bank Parameters	
Capacity *(Q_m)*	50 [A.h]
No. of module	25
Rated voltage	308 [V]
Internal resistance *(R_a)*	0.015 ± 25% [Ω]
Terminal resistance *(R_b)*	0.015 ± 25% [Ω]
Incipient capacitance *(C_i)*	3 [F]
polarization capacitance *(C_p)*	3 [F]
Minimum state of charge	70%
Maximum state of charge	80%
Current Controller Parameters	
k_p	3.7
k_i	23×10^{-3}
DC-link voltage Controller parameters	
$k_{p,dc}$	0.55
T_{idc}	2ms

In these conditions, the reference power of the battery bank changes for decreasing the input power to dc bus during voltage disturbances and fuzzy control strategy swatches the battery bank to the charging mode and battery's state of charge goes high. From Fig. 10 and Fig.11, it is evident that the FC system and battery bank together share this load requirement. Although the battery bank voltage is affected by the load conditions as seen in Fig. 12. As depicted in Fig.12, the battery voltage increases when the battery power is negative. In this condition, the battery's state of charge goes

high as shown in Fig.13. Fig. 14 shows the output voltage changes of fuel cell. The fuel cell voltage has not been affected during the voltage sag. The hydrogen flow rate varies according to the system power requirements as illustrated in Fig. 15. According to the simulation results in Figs. 14 and 15, it is clear that the parameters of fuel cell system has not changed during the occurring the voltage disturbances in distribution systems. These parameters are very important on the life time of fuel cell system. On the other hand, during the occurring voltage sag, the battery energy storage makes to improve the performance of the hybrid system. In this condition, the proposed power flow control strategy finds the suitable operating point for the battery and fuel cell power sources.

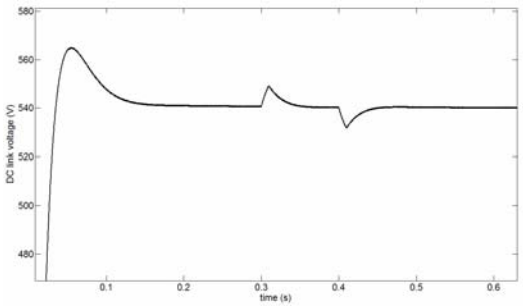

Fig. 8 Variations of DC link voltage during voltage dip.

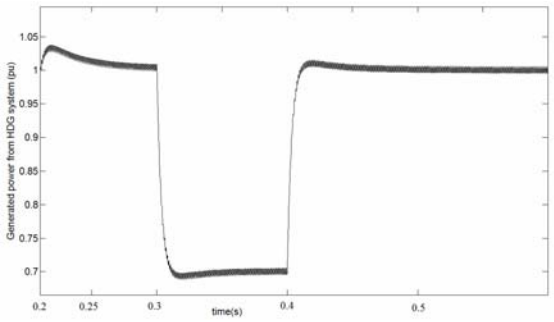

Fig. 9. Generated power from HDG system during voltage sag (p.u).

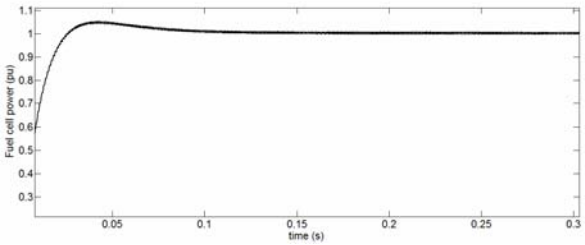

Fig.10.Variation of fuel cell power during voltage sag (p.u.)

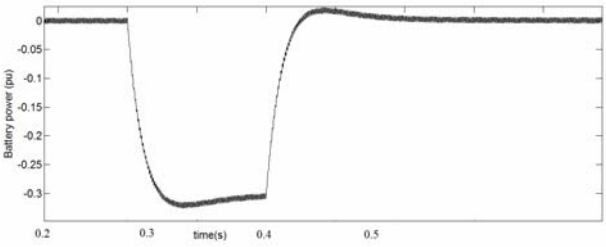

Fig.11.Variation of battery power during voltage sag (p.u.)

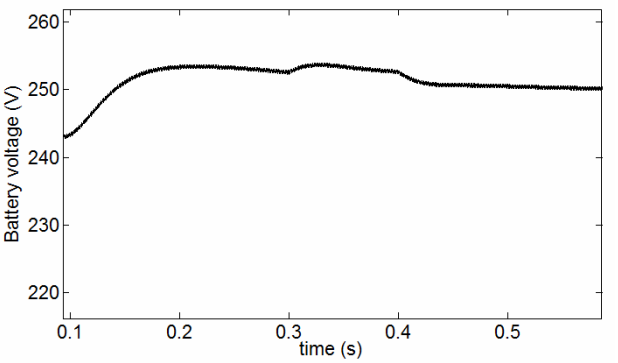

Fig.12. Variation of battery voltage during voltage sag.

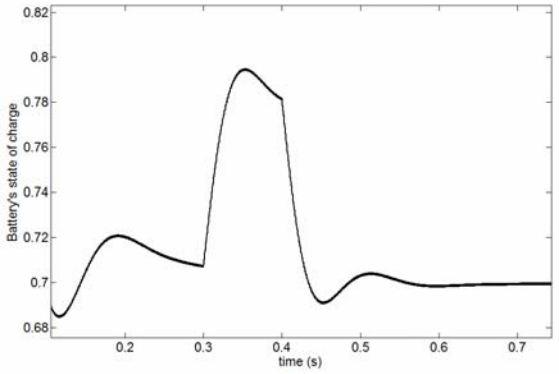

Fig.13. Battery's state of charge during voltage sag.

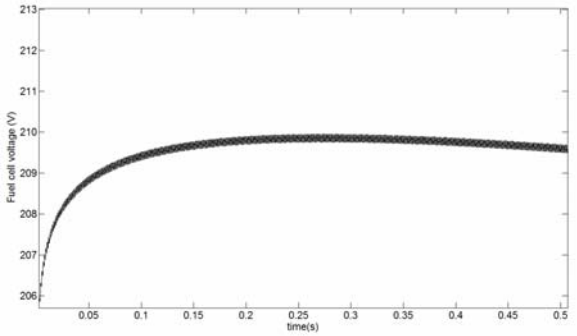

Fig.14. Variation of fuel cell voltage during voltage sag.

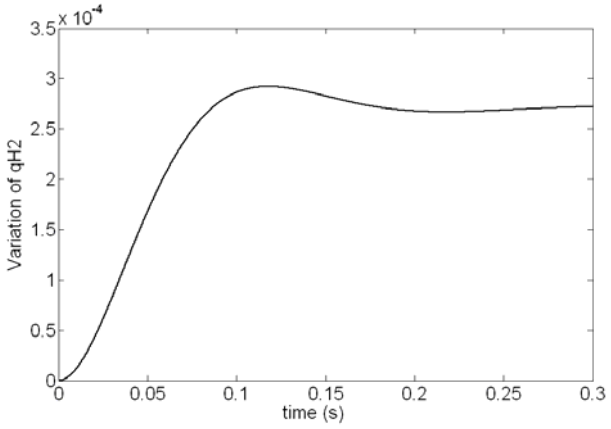

Fig.15. Variation of hydrogen molar flow during voltage sag.

VI. Conclusion

In this paper, the design of neuro fuzzy power flow control strategy has been investigated for hybrid fuel cell/ battery distributed generation system during the voltage disturbances in distribution systems. The proposed control strategy makes the hybrid system operates well under voltage sag conditions and could deliver the active power to load. Moreover, the local controllers of the fuel cell and power electronic devices guarantee the safe operation of them. Simulation results show the overall system performance including power control and voltage sag ride-through capability of the proposed control strategy.

References

[1] M. W. Ellis, M. R. Von Spakovsky, and D. J. Nelson, "Fuel cell systems: Efficient, flexible energy conversion for the 21st century," *Proc. IEEE*, vol. 89, no. 12, pp. 1808–1818, Dec. 2001.

[2] P.Thounthong, S.Raël, B.Davat, "Control Strategy of Fuel Cell and Supercapacitors Association for a Distributed Generation System", *IEEE Trans. Industrial Elec.*, vol. 54, pp.3225-3233, December 2007.

[3] L.Gao, Z. Jiang, R.A. Dougal, "Control Strategies for Active Power Sharing in a Fuel-Cell-Powered Battery-Charging Station", *IEEE Trans. Industry Applications*, vol. 40, pp.917-924.

[4] M.H.J. Bollen, "What is power quality?" *Electric Power Systems Research,* vol. 66, pp. 5-14, 2003.

[5] A.Hajizadeh, M.A.Golkar, "Intelligent Power Management Strategy of hybrid Distributed Generation System", *International Journal of Elec. Power and Energy Syst*. vol.29, pp.783-795, 2007.

[6] A.Hajizadeh, M.A.Golkar, "Improving voltage sag ride-through in hybrid fuel cell/ battery distributed generation systems", International Journal of Distributed Energy Resources, vol. 5 (1) pp.17-32, 2009.

[7] J. Padull´es, G. W. Ault, and J. R. McDonald, "An integrated SOFC plant dynamic model for power system simulation," J. Power Sources, pp. 495–500, 2000.

[8] Wang, L. X. "Back-Propagation of Fuzzy Systems as Nonlinear Dynamic System Identifiers", Proc. IEEE Int. Conf. on Fuzzy Systems, pp. 1409-1418, 1992, San Diego, CA.

[9] Ching-Hung Lee and Ching-Cheng Teng, "Identification and Control of Dynamic Systems Using Recurrent Fuzzy Neural Networks", IEEE TRANSACTIONS ON FUZZY SYSTEMS, VOL. 8, NO. 4, AUGUST 2000.